Proceedings of 2017 IEEE
International Conference on Mechatronics and Automation
August 6 - 9, Takamatsu, Japan

A Novel sEMG Control-based Variable Stiffness Exoskeleton

Yi Liu [*1], Shuxiang Guo [*2*3], Songyuan Zhang[*1] and Luc BOULARDOT[*1]

[*1] Graduate School of Engineering
[*2] Department of Intelligent Mechanical Systems Engineering
Kagawa University
Hayashi-cho, Takamatsu, 761-0396, Japan
s16g529@stu.kagawa-u.ac.jp

[*3] Key Laboratory of Convergence Medical Engineering System and Healthcare Technology,
The Ministry of Industry and Information Technology,
School of Life Science
Beijing Institute of Technology
Haidian District, Beijing, 100081, China
guo@eng.kagawa-u.ac.jp

***Abstract* –In recent years, surface electromyography (sEMG) signals which are biomedical signals generated by muscles have been utilized to estimate human's muscular torque and predict their intention. In this paper, a variable stiffness exoskeleton which utilizes EMG signals to adjust the stiffness of the output link to meet different environmental requirements and guarantee the wearer's safety has been proposed. There is a stiffness adjustment mechanism located on the forearm part of the exoskeleton. Two dry electrodes which collect sEMG signals from agonist and antagonist muscles pair were attached on the subject's skin of corresponding muscle fibers respectively. The collected sEMG signals could be utilized to adjust the stiffness of output link according to the subject's intention. Combining sEMG signals with variable stiffness actuator (VSA) in the proposed exoskeleton, different outputs of stiffness could be realized in a compact and light hardware system. Experimental results showed the stiffness could be adjusted smoothly according to the Intention-based sEMG control.**

Index Terms – Exoskeleton, Intention recognition, Surface electromyography, Variable stiffness

I. INTRODUCTION

With the increase of aged population in most country all over the world, the rate of stoke has a sustained growth [1]. Stroke, as a leading reason of disability, always causes partial destruction of cortical tissue and leads to a disorder of neural system. The incidence of hemiparesis which leads to the impairment of upper limb and disability of performing activities of daily living (ADL) after the outbreak of stroke is as high as 85% [2].Therefore, the demand for professional upper limb rehabilitation and support is inevitably increased. To relieve the burden of caregivers and support physicians to provide high-intensity therapy, robot-aided rehabilitation systems have been proposed in the past decades [3]-[15]. Compared with traditional physician therapy, robot-aided rehabilitation and training could realize concrete motor function evaluation based on the data such as residual voluntary joint force and muscle strength which collected by the sensors attached on the robot [16]. Besides, therapists could adjust the training rehabilitation plan according to those collected data from patients. Concerned clinical studies have verified the robot-assisted movement training based on rehabilitation robot could decrease impairment and improve strength compared with conventional therapy [17]. Especially, power-assist exoskeleton can enhance the strength for healthy people or recover the motor ability for post-stroke patients. Song et al. presented a home-based upper limb exoskeleton rehabilitation device (ULERD) which could provide two kinds of training mode respectively to meet the requirements of patients with different damage of motor function [9]. For the power-assisted exoskeleton, to guarantee enough torque to perform movement, there are mainly two kinds of compliant actuators: active and passive. In active compliant actuators, the compliance adjustment relies on proper sensors. Once these sensors failed, the safety of wearers cannot be guaranteed. Whereas, passive compliant actuators mainly rely on mechanical elastic elements to decouple the inertia of the motors from load so as to ensure the safety of users. Besides, the elastic elements could be used to store or release the kinetic energy. However, passive compliant actuators with constant stiffness cannot satisfy the requirements of complicated environments. Hence, the concept of variable stiffness has been proposed. The output stiffness can be adjusted according to the requirements imposed by a specific task and guarantee the safety of wearers. Various designs which aim at acquiring the ability of variable stiffness have been presented. VSA-II adopted the strategy that adjusts the pretension of the elastic elements so as to realize the aim of stiffness change [18]. Subsequently, vsaUT-II based on a variable transmission ratio lever arm has been proposed, which adopt elaborate structure design to avoid energy injection into or extraction from the internal elastic elements [19].

In recent years, sEMG signals were applied to predict the motions of subjects and estimate human muscular torque [20]-[23]. Power-assist exoskeleton could provide corresponding assistance on the basis of sEMG signals for disabled who've had serious arm injuries or enhance the endurance and strength for healthy people [24]. However, for the sEMG-based control, the troublesome issue we have to confront is the inherent characteristic of instability. Although some powerful algorithms and control strategies have been proposed and applied for upper limb exoskeleton to estimate muscular

torques from EMG activations [25]-[27], the complexity of signal processing is tricky with the increase of moving joints. To simplify the calibration procedures and improve the real-time response, Lenzi et al. proposed a proportional EMG control strategy applied in NEUROExos elbow skeleton [3] to give a rough estimate of the subject's muscular torque rather than accurate calibration. It indicated that the envelopes of sEMG signals could reflect the muscle activation level and the direction of the intended movement (e.g., flexion or extension) [28].

In this paper, a novel exoskeleton with variable stiffness based on sEMG signals control has been proposed. The main concept is to use sEMG signals to recognize the intention of the users so as to realize stiffness adjustment. The relationship between the wrist motions and user's intentions are pre-defined. Combining sEMG signals with stiffness adjustment in the novel exoskeleton, the internal mechanical compliance could be tuned according to the user's intentions so as to guarantee the safety and adapt different environments. The structure of this paper is organized by the following parts. The relative researches and the purpose of the research are represented in the first section. Then, a novel exoskeleton has been designed and relevant principle of stiffness variation has been introduced in Section II. Experimental results and analysis can be shown in Section III. Finally, conclusions and future work are given in Section IV.

II. Methods

A. The mechanical design

A VSA-based Exoskeleton device for elbow joint rehabilitation has been designed in the previous research of Guo. Lab [29]. It realized the stiffness adjustment by moving the pivot along the lever to achieve a variable transmission ratio between the internal elastic elements and the output link. However, limited by the single freedom of degree (elbow joint), it cannot guarantee an enough movement range to finish the preconceived action. Besides, it must be fastened on the table, which limits its application and degrades the comfort of wearers. To overcome the problems above and acquire high portability, a novel variable stiffness exoskeleton has been designed as shown in Fig. 1. There are 4 revolute joints to guarantee the exoskeleton move freely like the human joints without any limitation. And the link lengths of the exoskeleton could be matched to the subject's shoulder width and limb length thanks to the contribution of 2 prismatic joints. The main weight is allocated the main back-support frame, where the burden is shared by two straps tied on the shoulder. The exoskeleton is equipped with two brushes DC motors, one (Maxon RE-30 Graphite Brushes Motor) which coupled with a gearbox (Maxon Planetary Gearhead GP 32 C) is used for control the rotation angle of elbow joint by using cable, and the other (Maxon RE-13 Graphite Brushes Motor) which coupled with a gearbox (Maxon Planetary Gearhead GP 13 A) is used to change the positon of the pivot so as to adjust the stiffness for the output link. The motors are controlled by Maxon 50/5 ESCON controller. The motor and gearbox parameters could be seen in Table I and Table II.

TABLE I
Parameters of Motors

Motor	RE-30	RE-13
Type power	60 W	3 W
Nominal voltage	12 V	18 V
No load speed	7480 rpm	13000 rpm
Nominal torque	51.7 mNm	2.36 mNm

TABLE II
Parameters of Gearheads

Gearhead	GP 32 C	GP 13 A
Reduction	190:1	67:1
Max. continuous torque	6 Nm	0.3 Nm

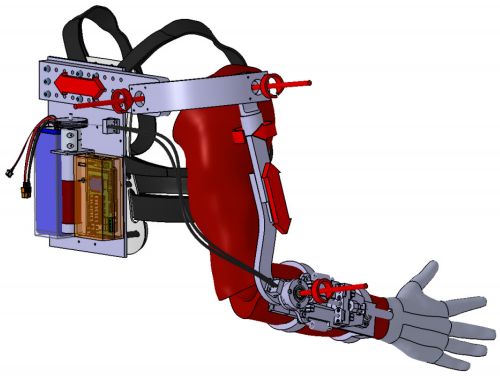

Fig. 1 The CAD model of the exoskeleton

B. The kinematic model

A sketch of the exoskeleton is shown in Fig. 2. It consists of 6 degrees of freedom, where 5 passive degrees of freedom to cater to the user's intention for spatial movement and one active degree of freedom actuated by cable to realize power-assist for elbow joint. In this exoskeleton, 4 revolute joints and 2 prismatic joints are designed to meet the requirement of kinematic performance. The four revolute movements include flexion/extension of shoulder and elbow joint, the pronation/ supination of the forearm and shoulder, whereas the two prismatic movements include the length adjustment of back and upper limb. The position of the first link was optimized for the purpose of maximizing the workspace of the shoulder joint and avoiding the interference between the exoskeleton and human joints. Link 2 is designed to satisfy the requirement of rotation for shoulder joint as the users wish. Link 3 could rotate between vertical to the ground and horizon to the ground when arm swing. Link 4 is designed to realize the pronation and supination for the upper limb. Link 5 is adjustable joint to guarantee accurate alignment between exoskeleton and human joints. Finally, Link 6 is the output link, the stiffness of which could be changed by moving the pivot along the lever. The Denavit-Hartenberg (D-H) parameters [30] of the exoskeleton are listed in Table III.

C. The working principle of variable stiffness mechanism

The forearm part consists of two parts: the stiffness adjustment mechanism and the output link which could be worn on the arm. They were linked together through a revolute

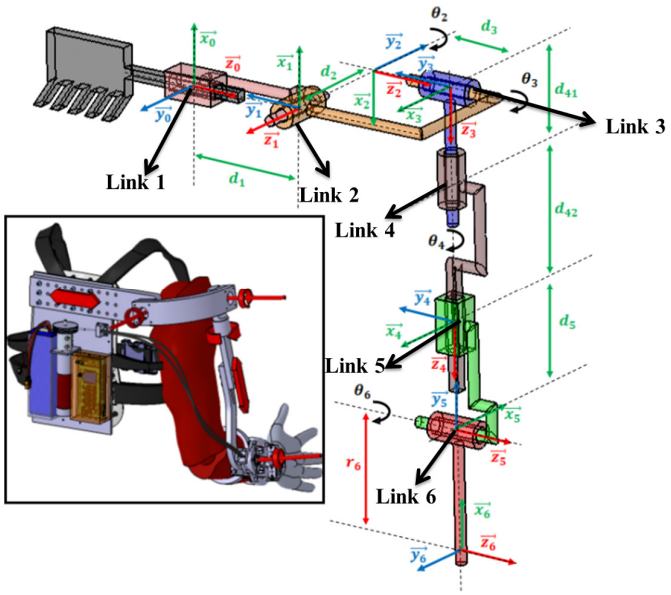

Fig. 2 Schematic of the kinematic model

TABLE III
D-H PARAMETERS

Link	θ_i	d_i	r_i	α_i
1	0	d_1(JV)	0	$-\pi/2$
2	$\pi+\theta_2$(JV)	d_2	0	$-\pi/2$
3	$-\pi/2+\theta_3$(JV)	d_3	0	$-\pi/2$
4	θ_4(JV)	$d_{41}+d_{42}$	0	0
5	π	d_5(JV)	0	$-\pi/2$
6	θ_6(JV)	0	r_6	0

※JV: Joint Variable

joint. Both of them could rotate together with the active elbow joint. The variable stiffness mechanism mainly consists of two elastic elements (tension springs), a DC motor, a ball screw, a lever and a main frame as shown in Fig. 3. Once the resistance force exceeds the threshold of the current stiffness, the output link will separate with the stiffness adjustment mechanism to protect the wearer's safety. The current threshold could be adjusted by the variable stiffness mechanism.

The definition of stiffness is as follows.

$$K = \frac{F}{\delta} \tag{1}$$

where K is the stiffness of the output link, F is the force exerted on the end of output link and δ is the output deflection along the orientation under the action of force.

The principle of stiffness adjustment is shown in Fig. 4. The forces generated by tension springs could be transmitted to the output link via the lever. A pivot could move along the slide rail. As long as the position of the pivot is changed, the transmission ratio of elastic elements versus output end will be changed as well. Based on the equilibrium of moments, to rotate the same deflection δ, the force exerted on the output end will be varied according to the transmission ratio. As a result, the characteristic of variation stiffness is realized. The CAD model and physical prototype could be seen in Fig. 5.

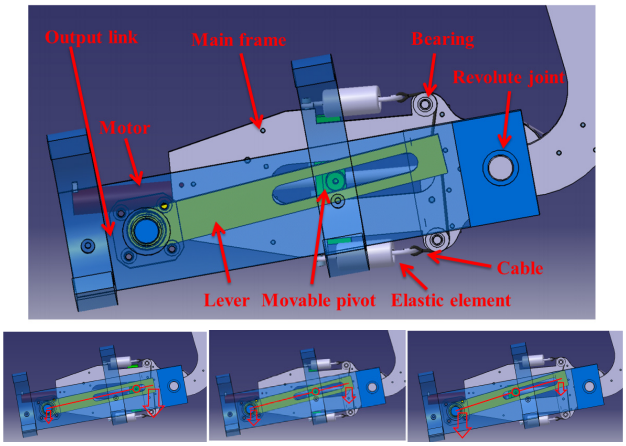

(a) Low stiffness (b) Medium stiffness (c) High stiffness

Fig. 3 Variable stiffness mechanism

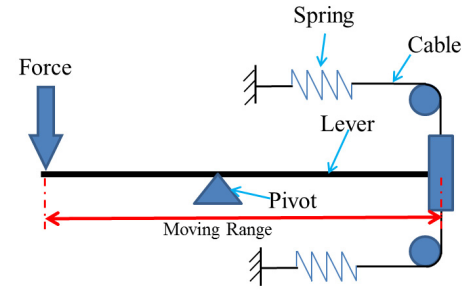

Fig. 4 Schematic of the working principle

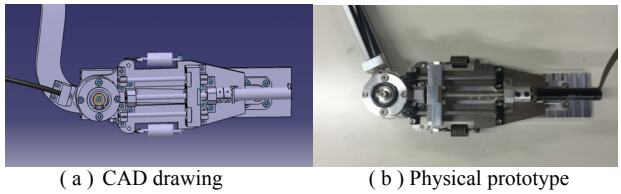

(a) CAD drawing (b) Physical prototype

Fig. 5 Variable stiffness mechanism

D. *Intention-based EMG control*

In the Intention-based EMG control strategy, we assumed that the subjects are healthy people who would like to enhance the endurance and strength or those patients who suffered from hemiplegia and have an intact upper-limb to carry out bilateral rehabilitation training for the purpose of recovering the normal movement ability of the impaired upper limb by using this exoskeleton. Considering cooperative motion of multi-joints could be time consuming and complicated, an Intention-based sEMG control based on motions of a single joint (wrist) has been proposed. The control strategy is easily implemented on the exoskeleton and suitable for different users to adjust the stiffness of the exoskeleton without long training and calibration time. The control diagram of stiffness adjustment is shown in Fig. 6. The agonist and antagonist muscles pair flexor carpi radialis (FCR) which mainly performs the function of the wrist flexion and extensor carpi radialis (ECR) which mainly performs the function of the wrist extension were set as the source of input variable. The raw sEMG signals generated from FCR and ECR separately

were collected by two dry electrodes. After corresponding signal processing, the filtered signals will be utilized to implement the intention recognition. In this segment, the intention of subject is divided into 4 kinds: intend to increase the stiffness, intend to decrease the stiffness, keep the stiffness or emergency. Those intentions are established relationship with related postures artificially. The classifier of intention recognition is illustrated as follows.

$$R = \begin{cases} 1, & (T_1 > T_{FCR}) \cap (T_1 > T_2) \\ 2, & (T_2 > T_{ECR}) \cap (T_2 > T_1) \\ 0, & (T_1 < T_{FCR}) \cap (T_2 < T_{ECR}) \\ -1, & else \end{cases} \quad (2)$$

where R is the result of identification which represented by numbers. T_1 is the value of sEMG signals generated by FCR, While T_2 is the value of sEMG signals generated by ECR. T_{FCR} and T_{ECR} represent the thresholds for judging wrist flexion and wrist extension respectively. Considering the risk of spasm, the motor will be stopped to ensure the user's safety when detect the abnormal signals.

Thus, the specific posture was utilized to express the subject's specific intention. Those postures are shown in Fig. 7. The relationship between wrist motions and stiffness trend are defined in Table IV.

III. Experiments and Analysis

A. sEMG collection and process

EMG signals are biological signals generated from motor neuron impulses, which are correlated with the physiological properties of concerned muscles. When collecting the EMG signals, an inevitable problem is the noise disturbance while travelling different tissues. For the purpose of obtaining the inherent characteristics hidden by noise, a powerful detection and filtering methodologies for sEMG processing is essential for the subsequent intention recognition. The flow chart of sEMG processing could be illustrated in Fig. 8. Most of external and artificial noises could easily be avoided by proper skin preparation (e.g. shave body hairs of participants and clean their skins with alcohols) and correct electrode position. After the proper skin preparation, dry electrodes were aligned parallel to the related muscles fibers and attached on the skin to collect raw sEMG signals. To avoid aliasing effects during sampling, the amplifier bandpass filter range from 10 Hz to 500 Hz with 1000 gain and 104 dB common mode rejection is adopted during sampling [31]. Then, all negative amplitudes will be converted to positive amplitudes by the procedure of full wave rectification. As an alternative to Moving Average and Root Mean Square smoothing, Butterworth filter is a typical digital filter with maximally flat frequency response in the passband. Compared with other digital filters, Butterworth filter has a more linear phase response in the passband. Given cut-off frequency ω_c=1, normalized Butterworth polynomials can be generalized as follows.

when n is even,

$$B_n(s) = \prod_{k=1}^{\frac{n}{2}} \left[s^2 - 2s\cos\left(\frac{2k+n-1}{2n}\pi\right) + 1 \right] \quad (3)$$

when n is odd,

$$B_n(s) = (s+1) \prod_{k=1}^{\frac{n-1}{2}} \left[s^2 - 2s\cos\left(\frac{2k+n-1}{2n}\pi\right) + 1 \right] \quad (4)$$

where n is the order of filter.

Higher order digital filters can be applied recursively to minimize the phase shift phenomenon [32]. Considering the balance between time lag and smoothness, a fourth-order low pass Butterworth filter was chosen to filter the signals in the experiments. The filtered signals will be used to intention recognition.

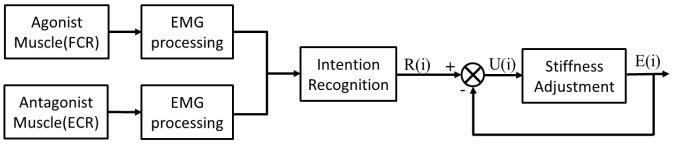

Fig. 6 Control diagram of stiffness adjustment
(R(i): Reference position U(i): Output positon E(i): Error between reference and output position)

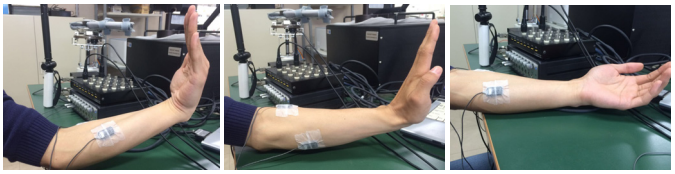

(a) Wrist flexion (b) Wrist extension (c) Relaxation

Fig. 7 Defined wrist postures

TABLE IV
THE RELATIONSHIP BETWEEN POSTURES AND STIFFNESS TREND

R	Posture	Stiffness trend
1	Wrist flexion	Increase
2	Wrist extension	Decrease
0	Relaxation	Remain
-1	Emergency	Stop motor

B. Experiments and results

The hardware of the system consists of an exoskeleton with stiffness adjustment mechanism, an EMG collector, an A/D board and a computer. The sEMG signals were collected

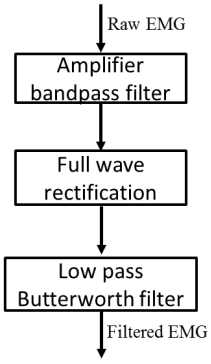

Fig. 8 The procedure of sEMG filtering

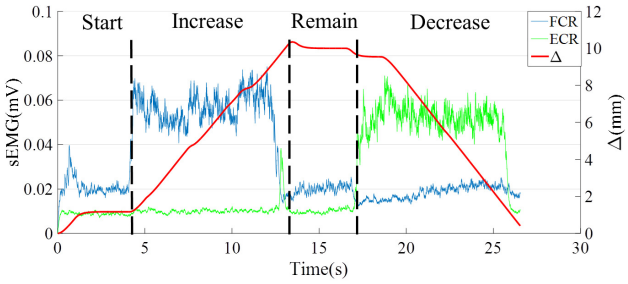

Fig. 9 sEMG signals and pivot position

(FCR: sEMG signals from flexor carpi radialis ECR: sEMG signals from extensor carpi radialis Δ : pivot moving distance of from the initial position)

by the EMG collection equipment (Personal-EMG, Oisaka Electronic Equipment Co. Ltd) with sampling rate 1000 Hz and recorded by an analog/digital (A/D) board (USB4716, Advantech Co. Ltd). The moving distance of pivot in the stiffness adjustment mechanism is displayed on the screen by a serial port output and recorded by a personal computer.

In the experiment, the subjects were asked to implement the related postures aforementioned to implement the stiffness adjustment. According to the difference of sEMG signals from the agonist (FCR) and antagonist (ECR) muscles pair, the wrist motion which the subject is performing could be recognized. When the sEMG activation of FCP is much higher than that of ECP and exceeds the correspondent threshold T_{FCP}, the motion is classified as wrist flexion. Further, the stiffness adjustment will move the pivot to increase the stiffness of output link. On the contrary, if the sEMG activation of ECP is much higher than that of FCP and exceeds the correspondent threshold T_{ECP}, the motion is classified as wrist extension. Thus, the mechanism will move the pivot inversely to decrease the stiffness of output link. In the case that both of them are lower than the respective thresholds and the difference between FCP and ECP is not so huge, the motion is classified as relaxation. Hence, the stiffness will be remained. In case of emergency situation occurs such as spasm, the motor will stop automatically to protect the subject's safety if abnormal sEMG signals are detected.

Considering individual difference between different people, the subjects were trained to use sEMG signals to control the stiffness adjustment mechanism and look for the optimal parameters for every subject in advance. The proposed Intention-based sEMG control was tested on 5 healthy male subjects for ten times respectively. At the beginning of experiments, the pivot in the stiffness adjustment mechanism is set at the beginning of the slide rail where is near to the elbow joint and has the characteristic of lowest stiffness. The initial position is defined as 0mm. The sEMG signals from a pair of agonist and antagonist muscles and the moving distance of pivot will be recorded simultaneously. Then, the subjects were informed to perform the motion of wrist flexion, relaxation, wrist extension successively to complete the variation of stiffness. The result of subject A can be seen in Fig. 9. The blue curve described the envelope of sEMG signals from FCR, while the green curve described the envelope of filtered sEMG signals from ECR. And the red curve represents the moving length from initial position. In the stages of increase and decrease, the intention of subjects could be recognized well. Although the difference between two sEMG signals is much larger in some situations, the position of the controlled pivot remains constant. It can be attributed to the inertia of the mechanism caused by high reduction ratio that make it response lag when change the status of motor. The similar results could be acquired from the other subjects.

Further, to verify the characteristic of stiffness variation, a force sensor (MINI 4/20, BL AUTOTEC. Ltd) was fastened on the end of output link. And an inertial sensor (MTx sensor, Xsens Technologies B.V.) was attached on the elbow joint of the exoskeleton. The exerted force on the end of output link and the rotation angle of elbow joint could be recorded simultaneously. The initial position of the pivot was set on the starting side of the slide rail where is near to the elbow joint. Three representative moving distances (0mm, 5mm, 10mm apart away from the initial position) to calculate the stiffness respectively. The experiment results are shown in Fig. 10. It can be obtained that the exerted force is nearly proportional to the deflection after the initial stage and the slope of each curve represents their respective stiffness K. Since the existence of friction between the main frame and the output link in the exoskeleton, it cannot be neglected in the initial stage because of the relative small exerted force. With the increase of the exerted force, the linear relationship between the deflection and the exerted force could be observed clearly. Besides, the longer the moving distance is, the more quickly the characteristic appears. It is due to that longer distance leads to higher stiffness. To rotate the same angle, the proportion of friction decreases rapidly in the case of high stiffness, and the linear feature appears early. According to the result, the variable stiffness has been realized. And the users could perform the power-assist or rehabilitation training with safe conditions by choosing suitable stiffness.

IV. Conclusions

In this paper, a novel sEMG Control-based variable stiffness exoskeleton was proposed. Compared with physical passive compliance which usually has a large value from inertia of the link, variable stiffness actuator could improve the performance of exoskeletons in different environment and guarantee the user's safety by properly adjusting the stiffness. In the proposed exoskeleton, the stiffness of output link could be adjusted according to the Intention-based sEMG control.

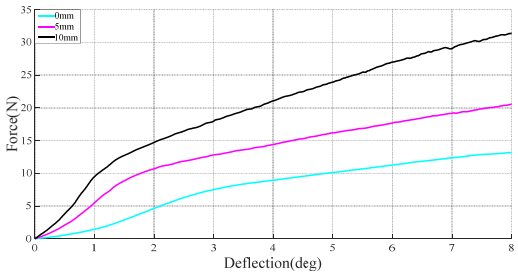

Fig. 10 Deflection versus output force

The sEMG signals were collected from the user's FCR and ECR and the intentions of subject could be recognized by the proposed sEMG-based control strategy. Therefore, the stiffness adjustment could be realized according to the user's intention while the stiffness of traditional VSA devices is tuned manually. The experiments have verified the validity of the proposed Intention-based sEMG control strategy for healthy people.

In the future, post-stroke patients who remained partial motor ability are expected to take part in the experiments to verify the effectiveness of stiffness adjustment for them. Furthermore, a sEMG-based torque estimation and power-assist control strategy will be considered to apply in the novel exoskeleton to enhance the endurance of healthy people or recover the motor ability of post-stroke patients.

ACKNOWLEDGMENT

This research is partly supported by National Natural Science Foundation of China (61375094), National High Tech. Research and Development Program of China (No.2015AA043202).

REFERENCES

[1] D. Mozaffarian, E. J. Benjamin, A. S. Go, D. K. Arnett, M. J. Blaha, M. Cushman*, et al.*, "Executive summary: Heart Disease and Stroke Statistics-2016 update: A report from the American Heart Association", *Circulation,* vol. 133, no. 4, p. 447, 2016.

[2] S. Barreca, S. L. Wolf, S. Fasoli, and R. Bohannon, "Treatment interventions for the paretic upper limb of stroke survivors: a critical review", *Neurorehabilitation and neural repair,* vol. 17, no. 4, pp. 220-226, 2003.

[3] N. Vitiello, T. Lenzi, S. Roccella, S. M. De Rossi, E. Cattin, F. Giovacchini*, et al.*, "NEUROExos: A powered elbow exoskeleton for physical rehabilitation", *IEEE Transactions on Robotics,* vol. 29, no. 1, pp. 220-235, 2013.

[4] S. S. Groothuis, G. Rusticelli, A. Zucchelli, S. Stramigioli, and R. Carloni, "The vsaUT-II: A novel rotational variable stiffness actuator", in *Proceedings of 2012 IEEE International Conference on Robotics and Automation (ICRA),* pp. 3355-3360, 2012.

[5] Z. Song, S. Guo, and Y. Fu, "Development of an upper extremity motor function rehabilitation system and an assessment system", International Journal of Mechatronics and Automation, vol. 1, no. 1, pp. 19-28, 2011.

[6] Z. Song, S. Guo, N. Xiao, B. Gao, and L. Shi, "Implementation of human-machine synchronization control for active rehabilitation using an inertia sensor", *Sensors*, vol. 12, no. 12, pp. 16046-16059, 2012.

[7] Z. Song and S. Guo, "Design process of exoskeleton rehabilitation device and implementation of bilateral upper limb motor movement", *Journal of Medical and Biological Engineering*, vol. 32, no. 5, pp. 323-330, 2012.

[8] M. Pang, S. Guo, and Z. Song, "Study on the sEMG driven upper limb exoskeleton rehabilitation device in bilateral rehabilitation", *Journal of Robotics and Mechatronics*, vol. 24, no.4, p. 585, 2012.

[9] Z. Song, S. Guo, M. Pang, S. Zhang, N. Xiao, B. Gao, et al., "Implementation of resistance training using an upper-limb exoskeleton rehabilitation device for elbow joint", *Journal of Medical and Biological Engineering*, vol. 34, no. 2, pp. 188-196, 2014.

[10] H.-S. Park, Q. Peng, and L.-Q. Zhang, "A portable telerehabilitation system for remote evaluations of impaired elbows in neurological disorders", *IEEE Transactions on Neural Systems and Rehabilitation Engineering,* vol. 16, no. 3, pp. 245-254, 2008.

[11] X. Tang, Y. Liu, C. Lv, and D. Sun, "Hand motion classification using a multi-channel surface electromyography sensor", *Sensors,* vol. 12, no. 2, pp. 1130-1147, 2012.

[12] S. Zhang, S. Guo, M. Pang, and M. Qu, "Training model-based masterslave rehabilitation training strategy using the phantom Premium and an exoskeleton device", in *Proceedings of 2014 International Conference on Complex Medical Engineering*, pp. 26-29, 2014.

[13] S. Zhang, S. Guo, B. Gao, H. Hirata, and H. Ishihara, "Design of a Novel Telerehabilitation System with a Force-Sensing Mechanism", *Sensors*, vol. 15, no. 5, pp. 11511-11527, 2015.

[14] S. Zhang, S. Guo, Y. Fu, L. Boulardot, Q. Huang, H. Hirata, et al., "Integrating Compliant Actuator and Torque Limiter Mechanism for Safe Home-Based Upper-Limb Rehabilitation Device Design", *Journal of Medical and Biological Engineering*, vol. 37, no. 3, pp. 357-364, 2017.

[15] Y. Zhang, S. Guo, G. Cao, S. Zhang, and Y. Liu, "A novel variable stiffness actuator-based exoskeleton device for home rehabilitation", in *Proceedings of 2016 IEEE International Conference on Mechatronics and Automation (ICMA)*, pp. 878-883, 2016.

[16] G. Kwakkel, B. J. Kollen, and H. I. Krebs, "Effects of robot-assisted therapy on upper limb recovery after stroke: a systematic review", *Neurorehabilitation and neural repair,* vol. 22, no. 2, pp. 111-121, 2008.

[17] S. Hesse, G. Schulte-Tigges, M. Konrad, A. Bardeleben, and C. Werner, "Robot-assisted arm trainer for the passive and active practice of bilateral forearm and wrist movements in hemiparetic subjects", *Archives of physical medicine and rehabilitation,* vol. 84, no. 6, pp. 915-920, 2003.

[18] R. Schiavi, G. Grioli, S. Sen, and A. Bicchi, "VSA-II: A novel prototype of variable stiffness actuator for safe and performing robots interacting with humans", in *Proceedings of 2008 IEEE International Conference on Robotics and Automation (ICRA)*, pp. 2171-2176, 2008.

[19] S. S. Groothuis, G. Rusticelli, A. Zucchelli, S. Stramigioli, and R. Carloni, "The variable stiffness actuator vsaut-ii: Mechanical design, modeling, and identification", *IEEE/ASME Transactions on Mechatronics,* vol. 19, no. 2, pp. 589-597, 2014.

[20] S. Zhang, S. Guo, B. Gao, Q. Huang, M. Pang, H. Hirata*, et al.*, "Muscle Strength Assessment System Using sEMG-Based Force Prediction Method for Wrist Joint", *Journal of Medical and Biological Engineering,* vol. 36, no. 1, pp. 121-131, 2016.

[21] M. Pang, S. Guo, Q. Huang, H. Ishihara, and H. Hirata, "Electromyography-Based Quantitative Representation Method for Upper-Limb Elbow Joint Angle in Sagittal Plane", *Journal of Medical and Biological Engineering,* vol. 35, no. 2, pp. 165-177, 2015.

[22] S. Guo, M. Pang, B. Gao, H. Hirata, and H. Ishihara, "Comparison of sEMG-based feature extraction and motion classification methods for upper-limb movement", *Sensors*, vol. 15, no. 4, pp. 9022-9038, 2015.

[23] Z. Song, S. Guo, M. Pang, and S. Zhang, "Recognition of motion of human upper limb using semg in real time: Towards bilateral rehabilitation", in *Proceedings of 2012 IEEE International Conference on Robotics and Biomimetics (ROBIO)*, pp. 1403-1408, 2012.

[24] R. Gopura, D. Bandara, J. Gunasekara, and T. Jayawardane, "Recent trends in EMG-Based control methods for assistive robots", *Electrodiagnosis in new frontiers of clinical research,* pp. 237-268, 2013.

[25] K. Kiguchi, T. Tanaka, and T. Fukuda, "Neuro-fuzzy control of a robotic exoskeleton with EMG signals", *IEEE Transactions on Fuzzy Systems,* vol. 12, no. 4, pp. 481-490, 2004.

[26] E. E. Cavallaro, J. Rosen, J. C. Perry, and S. Burns, "Real-time myoprocessors for a neural controlled powered exoskeleton arm", *IEEE Transactions on Biomedical Engineering,* vol. 53, no. 11, pp. 2387-2396, 2006.

[27] C. Fleischer and G. Hommel, "A human--exoskeleton interface utilizing electromyography", *IEEE Transactions on Robotics,* vol. 24, no. 4, pp. 872-882, 2008.

[28] T. Lenzi, S. M. M. De Rossi, N. Vitiello, and M. C. Carrozza, "Intention-based EMG control for powered exoskeletons", *IEEE Transactions on Biomedical Engineering,* vol. 59, no. 8, pp. 2180-2190, 2012.

[29] S. Zhang, S. Guo, M. Pang, B. Gao, and P. Guo, "Mechanical design and control method for sea and VSA-based exoskeleton devices for elbow joint rehabilitation", *Neuroscience and Biomedical Engineering,* vol. 2, no. 3, pp. 142-147, 2014.

[30] B. Siciliano and O. Khatib, *Springer handbook of robotics[M]*. Springer, 2016.

[31] S. Guo, Y. Liu, Y. Zhang, S. Zhang, and K. Yamamoto, "A VR-based self-rehabilitation system", in *Proceedings of 2016 IEEE International Conference on Mechatronics and Automation (ICMA)*, pp. 1173-1178, 2016.

[32] P. Konrad, "The abc of emg", *A practical introduction to kinesiological electromyography,* vol. 1, pp. 30-35, 2005.